ADIBEAM: Adaptive Digital Beamforming for Galileo Reference Ground Stations

Jose Lopez Vicario[1], Felix Antreich[2], Marc Barcelo[1], Nikola Basta[2], Joan Manuel Cebrian[3], Manuel Cuntz[2], Oscar Gago[4], Laura Gonzalez[4] , Marcos V.T. Heckler[2], Cristina Lavin[4], Marti Mañosas[1], Joan Picanyol[3], Gonzalo Seco-Granados[1], Matteo Sgammini[2], Francisco Amarillo[5]
[1]*Universitat Autonoma de Barcelona (UAB), Spain,* [2]*Deutsches Zentrum für Luft- und Raumfahrt (DLR), Germany,*
[3]*Indra Espacio, Spain,* [4]*TTI, Spain,* [5]*European Space Agency (ESA), The Netherlands*

BIOGRAPHY

Dr. Jose Lopez Vicario is Assistant Professor at Universitat Autonoma de Barcelona (UAB). His current activities focus on array signal processing for Galileo systems and cooperative positioning. He received his Ph.D. in Electrical Engineering from Universitat Politecnica de Catalunya (UPC).

Felix Antreich (IEEE M06) received the diploma in electrical engineering from the Munich University of Technology (TUM), Munich, Germany, in 2003, where he is currently pursuing the Ph.D. degree in electrical engineering. Since July 2003, he has been with the Institute of Communications and Navigation of the German Aerospace Center (DLR), Wessling Oberpfaffenhofen, Germany.

Marc Barcelo Llado is Research Assistant at Universitat Autonoma de Barcelona (UAB) within the Signal Processing for Communications and Navigation (SPCOMNAV) group. His research interests are cooperative communications and distributed beamforming. He received his M.Sc. in Electrical Engineering in 2010 from Universitat Autonoma de Barcelona (UAB).

Nikola Basta graduated with the degree in telecommunications engineering at the School of Electrical Engineering at the University of Belgrade. In 2008 he joined the antenna group of the DLRs Institute of communications and navigation where he is involved in the design and analysis of microstrip antenna arrays.

[0]THE WORK REPORTED IN THIS ARTICLE HAS BEEN SUPPORTED UNDER A CONTRACT OF THE EUROPEAN SPACE AGENCY (ADIBEAM AO/1-5934/08/NL/AT). THE VIEWS PRESENTED IN THE PAPER REPRESENT SOLELY THE OPINION OF THE AUTHORS AND SHOULD BE CONSIDERED AS R&D RESULTS NOT NECESSARILY IMPACTING THE EGNOS AND GALILEO SYSTEM DESIGN. THE WORK OF THE UAB MEMBERS HAS BEEN ALSO SUPPORTED BY THE SPANISH GOVERNMENT UNDER PROJECT TEC2008-06305, THE CATALAN GOVERNMENT UNDER GRANT 2009 SGR 298, AND THE CHAIR OF KNOWLEDGE AND TECHNOLOGY TRANSFER PARC DE RECERCA UAB - SANTANDER. J.L. VICARIO AND G. SECO-GRANADOS ARE ALSO AFFILIATED WITH IEEC-UAB.

Joan Manuel Cebrian received the Telecommunication Engineer degree from the Universitat Politcnica de Catalunya (UPC). Currently he is in charge of Research and Developments initiatives of the Communications and Navigation Solutions Department in Indra Espacio Barcelona. He has been Project Manager and Technical Responsible of different projects in satellite communications field for more than 15 years in the frame of ESA, EU and National framework programs.

Manuel Cuntz received the diploma in electrical engineering degree in 2005 from the Technical University of Kaiserslautern. He joined the Institute of Communications and Navigation of DLR in 2006. His fields of research are satellite navigation receivers.

Oscar Gago received his Degree in Technical Telecommunications Engineering, speciality in Electronic Systems, by the University of Cantabria (Spain) in 2007. Since then, he has been working as an Antenna Design Engineer at TTI (Spain) in the Antennas Department. His research interests are focused on the design of antennas for MIMO systems and mobile terminals.

Laura Gonzalez received her degree in physics and electronics from the University of Cantabria. Since 1999 she has been working as an antennas engineer at TTI Norte in Santander. Her present work is focused on the design and investigation of broadband printed antennas and phase scan arrays for broadband mobile communications.

Marcos V. T. Heckler was born in Rio Grande, Brazil, in 1978. He received the B.Sc. degree in Electrical Engineering (Emphasis in Electronics) in 2001 from Universidade Federal de Santa Maria (UFSM), Brazil, the MSc. degree in Electronic Engineering (Microwaves and Optoelectronics) in 2003 from Instituto Tecnolgico de Aeronautica (ITA), Brazil, and the doctoral degree in Electrical Engineering in 2010 from Technische Universitat Munchen (TUM), Germany. From April to August 2003 he worked as a Research Assistant with the Antennas and Propagation Laboratory (LAP) at ITA. From October 2003 to June 2010, he worked as a Research Associate with the Antenna Group, Institute of Communications and Navigation, German Aerospace Center (DLR). Since June 2010, he is an Assistant Professor at Universidade Federal do Pampa (UNIPAMPA), in Alegrete - RS, Brazil. His current research interests are the design of microstrip antennas and arrays and the development of numerical techniques for microstrip antennas.

Cristina Lavin received her degree in Telecommunications Engineering from the University of Cantabria. From then, she has been working as an Antenna Engineer at TTI Norte. Her current activities are focused on the design and develope of electronically scanned phased arrays for broadband mobile communications.

Marti Mañosas Caballu received the M.Sc. in Electrical Engineering in 2009 from Universitat Autonoma de Barcelona (UAB). He started his PhD studies in March 2009 at UAB, where he is currently working as a Research Assistant within the Signal Processing for Communications and Navigation (SPCOMNAV) group. His research interests are in the field of statistical signal processing for communications and navigation.

Joan Picanyol received the Telecommunications Engineer degree from the Universitat Politecnica de Catalunya (UPC). Currently he is working in Indra Espacio and actively implicated in diverse projects involving a high degree of distributed system interoperability. He is expert in redundant and high-availability platforms using Unix and J2EE technologies.

Gonzalo Seco-Granados is Associate Professor in the Telecommunications and Systems Eng. Dept. of the Univ. Autnoma de Barcelona (Spain) since Jan. 2006. From 2002-2005, he was staff member at the Radionavigation Section in ESTEC/ESA, where he was involved in the Galileo project and in the development of GPS receivers and applications. He received his PhD degree in electrical engineering from the Univ. Politcnica de Catalunya in 2000. He is currently Director of the UAB-Santander Chair of Technology Transfer.

Matteo Sgammini received the BEng degree in telecommunication engineering from the Universit Politecnica delle Marche (UNIVPM), Ancona, Italy, in 2002 and the MEng degree in and electrical engineering from the Universit degli Studi di Perugia, Perugia, Italy, in 2005. From January 2005 to August 2008 he worked as system/software engineer at MTU Aero Engine, Munich, Germany. Since September 2008, he has been with the Institute of Communications and Navigation of the German Aerospace Center (DLR), Wessling Oberpfaffenhofen, Germany.

Francisco Amarillo works for ESA in the design of the navigation and integrity algorithms for the Galileo IOV/FOC Ground Mission Segment. He received his Masters Degree in Telecommunication by the Polytechnic University of Madrid (UPM) Spain in 1997, and his Masters Degree in Surveying Engineering by the Polytechnic University of Madrid (UPM) Spain in 1992. He has been working for the Galileo Programme of ESA since 2001 and leads numerous research activities within the ESA Technical Directorate.

ABSTRACT

Navigation accuracy and integrity demanded by Galileo and its future evolution motivate the study and design of advance receiving techniques. In that direction, the ADIBEAM project focus on the design of high accuracy ground stations. More specifically, the project deals with the adoption of advance receivers based on the use of arrays of antennas and digital beamforming.

In this paper, we present the receiver solution proposed in the project. This solution has been designed aimed at addressing the problems arising when an array of antennas is implemented in practice. Basically, the main problem is the extreme difficult to perfectly control and calibrates all the components of the system. For that reason, a realistic Experimentation Platform has been developed. This platform is based on the software emulation of all the components of the system and the implementation of a GNSS software receiver based on digital beamforming. Concerning the beamforming solutions, robust approaches have been proposed in order to cope with array perturbations.

As revealed by the results obtained in the project, the proposed receiver architecture based on the adoption of an antenna array is able to attain code centimetre and carrier millimetre accuracy in challenging scenarios with multipath, interference and scintillation effects.

INTRODUCTION

The ADIBEAM project is an European Space Agency (ESA)-funded project aimed at designing high accuracy ground stations. In the context of the Galileo Ground Mission Segment, tracking stations achieving centimetre level tracking accuracy are required to provide the system with accurate satellite ephemeris and clock prediction models [1]. The motivation of such objective comes from the navigation accuracy and integrity demanded by Galileo and its future evolution. The improvement of the accuracy of the ground station would have an extraordinary impact in the whole system because the same overall system performance could be obtained with less ground stations, thus having a substantial favourable effect of system cost and operations complexity. Similarly, if the number of ground stations is maintained, enhanced stations will have lead to an improved system performance.

The objective of the project, in particular, is to achieve cm and mm accuracy in terms of code and carrier tracking errors, respectively. Tracking stations work in static and partially controlled scenarios, being multipath and interference components the dominant error sources. One of the most promising approaches to cope with multipath and interference signals is the adoption of arrays of antennas at the ground station receivers [2, 3]. Besides, the array gain provided by such kind of solution may be also useful to alleviate the signal power loss induced by ionospheric scintillation. In that direction, the adoption of ground station receivers based on the use of an array of antennas is considered. This project, in particular, focuses on the adoption of digital beamforming and the work carried out considers the design of the complete receiver architecture and functionalities, including both the hardware and software components (antennas, RF chains, GNSS software receiver and digital beamforming), and the development of a representative software-based experimentation platform.

The main problem arising when an antenna array is implemented in practice is the extreme difficult to perfectly control and calibrates all the components of the system. Typical array perturbations are due to the non-ideal response of the hardware elements (antenna and RF chains) [3, 4, 5], mutual coupling effects, cross-polarization coupling, antenna position errors, etc. Indeed, the array performance is quite sensitive to these perturbations, showing dramatic performance losses if these are not carefully addressed. For that reason, this paper gives special emphasis to this issue by:

- designing an array of antennas based on a rectangular deployment of planar antennas. The motivation of such option comes from the fact that this is a feasible and ready-to-use solution for practical implementation thanks to the reproducibility of antenna conditions, ease of calibration and manufacturing, etc.
- introducing an online (real-time) calibration mechanism aimed at compensating the spurious differences between the receiver composite channels and the nominal parameters. The proposed mechanism allows for the simultaneous operation of the GNSS receiver and the calibration (i.e., the calibration can be performed while the GNSS receiver is running and tracking satellite signals).
- proposing robust digital beamforming techiques able to cope with the spurious perturbations and the particular difficulties associated with the signal scenario in ground stations (such as the presence of coherent reflections and the need to track satellites at low elevations).

Concerning the digital beamforming solutions, some misconceptions drive the designers to propose non-adequate solutions such as the well-known Capon and MMSE beamformers [3]. These solutions are useful for communication systems but some problems appear when these are applied on the navigation context. On one hand, the Capon solution is quite sensitive to multipath (coherent) components as the beamformer compensates all the contributions in order to minimize total output power (i.e., LOSS signal is cancelled). On the other hand, MMSE beamformer, tends to (constructively) combine the multipath components with the signal of interest. As a consequence, the propagation delay of the LOSS signal cannot be accurately obtained. In this work, however, we propose novel beamforming solutions. First, a deterministic approach based on an iterative procedure is presented. The proposed beamformer obtains better results than those attained with the classical deterministic delay-and-sum and Dolph-Chebychev solutions presented in other related projects and research works. Besides, it provides a high flexibility in terms of array gain vs. sidelobe attenuation trade-offs and the possibility of tailoring the beampattern to specific scenarios. Furthermore, an adaptive beamformer based on the Iterative Adaptive Approach (IAA) [6] is also proposed. Differently from other adaptive beamformers presented in the literature, the presented robust beamformer is intrinsically capable of filtering coherent signals.

Finally, the system proposed in the Project is validated by a complete and realistic Experimentation Platform. More specifically, this platform is based on the software emulation of all the components of the system (received signals, antennas and RF chains response, etc.) and the implementation of a GNSS software receiver based on digital beamforming. The signal generator accurately reproduces the effects caused by real RF hardware. In order to test the robustness of the proposed digital beamforming, different perturbation sources are induced in the system.

ADIBEAM SCENARIO

In ADIBEAM project, the design of the GNSS receiver for Galileo Reference Ground Stations is considered. The main objective of such design is to achieve cm and mm accuracy for both the DLL and PLL tracking. In particular, we focus on achieving such requirements by tracking Safety-of-Life signals (pilots on L1 and E5b). Since the main sources of errors in such scenario are ionospheric scintillation, multipath and interference, the use of an array of antennas at the receiver is adopted. In particular, the scenario of the project is the following:

- The ionospheric conditions correspond to a Sun Spot number equal to 140.
- The direction-of-arrival (DOA) of the LOSS is perfectly known at the receiver.
- Four multipath components in the scenario with the following parameters:
  - Multipath powers modeled as Gamma random variables (r.v.) with m=30 and average LOSS signal-to-multipath ratio equal to:
    - o SMR_1=9dB, SMR_2=6dB, SMR_3=6dB, SMR_4=9dB.

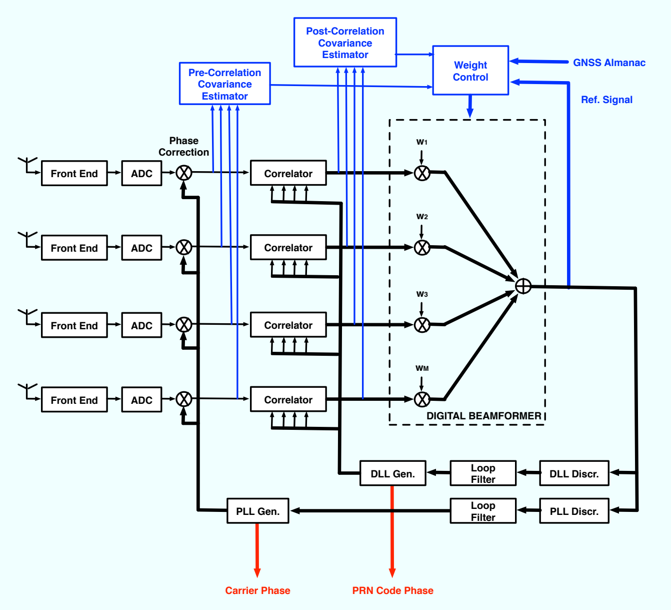

Fig. 1 Receiver Architecture based on Antenna Array.

- Multipath phases modeled as uniform r.v. between $-\pi$ and π.
- Multipath delays equal to:
  - o T_{MP_1}=0.25ns, T_{MP_2}=0.5ns, T_{MP_3}=0.75ns, T_{MP_4}=1ns.

- Two in-band interference sources with bandwidth equal to 1 KHz and 1 MHz and power equal to P_{i1}= -115 dBW and P_{i2}= -110dBW, respectively.
- The multipath and interference signals can only arrive with elevations equal or lower than 7.5°.

PROPOSED ARCHITECTURE

An overview of the general architecture of the GNSS receiver and the implementation of the digital beamforming is depicted in Figure 1. Next, we present in detail the different blocks of the proposed architecture.

Antenna and Array structure

The main advantages of using antenna arrays for the reception of GNSS signals is the possibility to suppress interference by introducing nulls in the directions where these come from and simultaneously to point the main beam in the desired direction. This improves the signal-to-noise and the signal-to-interference ratios of the whole system.

Microstrip antennas are very suitable for the proposed application, due to their low aerodynamic profile, ease of construction and low cost. Moreover, other passive circuits can also be implemented in microstrip technology and directly integrated in the antenna, saving costs, weight and space [7].

For this application, two stacked patches have been used to obtain the dual-band response. The top patch resonates in the higher frequency band, while the bottom patch operates at the lower frequency band. The dielectric materials have been chosen in order to achieve wide radiation patterns while maintaining good radiation efficiency. The proposed quadruple feeding with sequential phase weighting yields good RHCP polarization characteristics. The stack-up and architecture of the antenna is shown in the Fig. 2 whereas the feeder is depicted in Fig. 3.

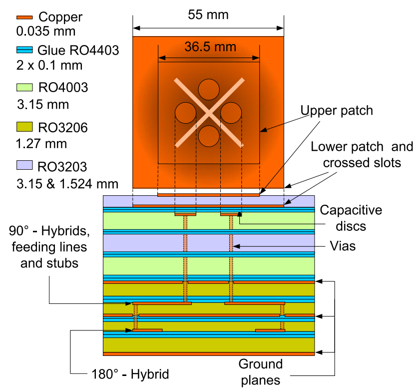

Fig. 2 Stack-up and architecture of the antenna.

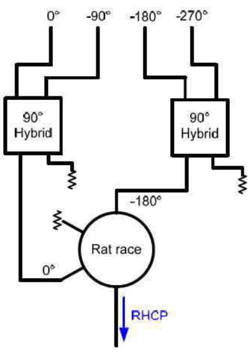

Fig. 3 Feeding Network of each antenna element.

The design of the antenna array started by the definition of the array configuration and the array size. These properties depend on the radiation characteristics of the single radiating element and they were fixed taking into account the performance of the overall antenna (mainly in terms of gain when the main beam points towards low elevation angles) and the manufacturing process.

The increase in the array size makes possible to scan the beam further besides increasing the gain. However, making the array too large can also bring several disadvantages. Especially by employing beamforming techniques, the increase in the number of array elements causes the increase in the number of signal channels, hence demanding more processing capability. This is especially critical if the beamforming should be done in real-time. Therefore, a compromise between these factors should be found in order to define the final array size.

The proposed array configuration is a 2-dimensional array of 6x6 elements in a rectangular structure. The distance between elements in both directions is 95 mm. This antenna array size meets the required antenna specifications. Besides this configuration with an even number of antenna elements reduces the complexity of the feeding network and therefore, the manufacturing cost is lower. Fig. 4 shows the antenna array configuration.

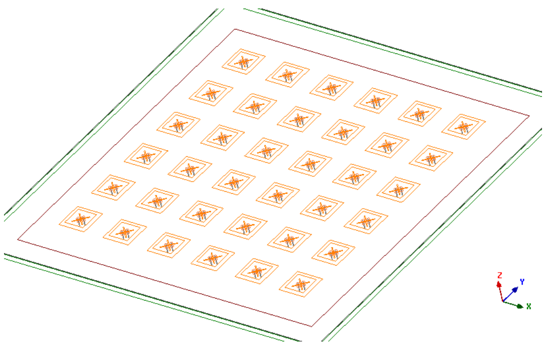

Fig. 4 Layout of the 6x6 antenna array.

RF chains and ADC

The receiver shall acquire and track L1 and E5b signals from the Galileo satellites associated with SoL as described in GALILEO ICD. For that reason the passive antenna of the receiving system is directly connected to an RF-board which contains a Diplexer to separate the L1 and E5b bands. One LNA for each band and a first band-pass filter for out of band interference suppression are used for a first signal conditioning. Fig. 5 shows a schematics of the active antenna part, which is needed for each single antenna element.

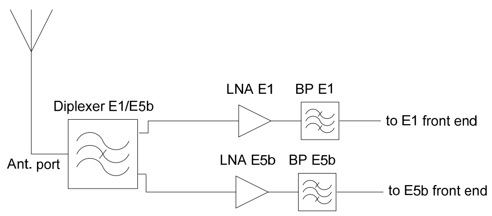

Fig. 5 Active antenna.

Subsequently the amplified and filtered RF signals are fed to the frontend boards. The front ends for further amplification and down conversion are physically separated from the antenna array. The conventional low IF super heterodyne architecture, which was chosen for this project, is state of the art and can be well described by existing models. The incoming signal is first amplified in two stages and enters subsequently the mixing stage. The RF signal is mixed down to a low intermediate frequency. A low-pass filter eliminates the RF and LO breakthrough signals of the mixer. The signal is then amplified again by two stages and filtered by a band-pass anti aliasing filter. This band-pass filter allows subsampling the IF signal and thus reduce the sampling rate. Before the signal enters the ADC it passes a variable gain amplifier to adjust the right power level. The ADC uses 14-Bit to sample the IF signal. This results in a effective dynamic range of more 65 dB which is needed to transfer the received signal containing interference to the digital domain without loss of information. Fig. 6 shows a blockdiagram of the front end architecture.

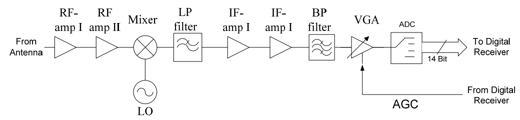

Fig. 6 Front End Blockdiagram with band-pass sampling.

Digital Beamforming

As shown in Figure 1, the design is following the approach of so-called post-correlation beamforming, i.e., digital beamforming is applied to digital samples at the output of the bank of correlators. This solution provides a good trade-off in terms of flexibility and complexity. This is because post-correlation allows implementing different beamforming algorithms in a flexible manner by adopting a software implementation and the beamforming weights have to be applied for much smaller rates than for pre-correlation beamforming implementation. Besides, it can be easily shown that the complexity of both pre-correlation and post-correlation beamforming is of the same magnitude.

By adopting the post-correlation solution, we need a different digital beamformer for each satellite and frequency band. In order to provide a clear picture of the proposed solution, we have restricted the architecture representation to cover only one of these digital beamformers. Indeed, we also consider such restriction in the sequel (especially in the digital beamformers description) for the ease of notation.

As previously commented, we propose different digital beamforming algorithms (deterministic and adaptive). Further details will be provided next but, however, it is worth pointing out here that adaptation of the adaptive solution will be based on the covariance measurements at pre- and/or post-correlation levels. Thus, the spatial covariance matrix needs to be estimated pre- or post-correlation and to be introduced to the beamforming algorithms (as observed in Fig. 1). An estimate of the spatial covariance matrix at the pre-correlation level can be considered as an estimate of the noise-plus-interference spatial covariance matrix.

GNSS Receiver

The proposed GNSS receiver architecture is also presented in Figure 1 and can be summarized as follows:

- Tight integration with the beamformer where:
  1. Code correlators are placed before the beamfoming module (with the same frequency correction and time reference for all the antennas).
  2. Tracking loops are placed at the output of the beamforming module.
- Adoption of conventional acquisition and tracking blocks. As for the tracking blocks, the following DLL and PLL blocks are considered:
  1. A first order dot-product DLL with E-L spacing equal to 0.1 chips and bandwidth equal to 0.2 Hz.
  2. A second order arctangent PLL with bandwidth equal to 3 Hz.

The justification from such design solution is based on two premises:

- A tight integration with the beamformer is necessary in order to fully exploit the advantages of a multi-antenna receiver. That is to say, the beamformer and the receiver cannot be considered as independent units. Although this would have the benefit that a conventional receiver could be used, there would be serious performance limitations as only very simplistic pre-correlation beamformers would be possible.
- In spite of the tight integration, it is desired to build the receiver using the blocks usually found in conventional receivers, without changing their implementation, only their number and arrangement. The optimization of these blocks, such as the correlators and the tracking loops, has been carried out with great detail by the manufacturers. The fact that the design of such blocks need not be changed would pave the way for the adoption of antenna array technology by GNSS receiver manufacturers.

Concerning the parameters selected for the tracking loops, such selection is aimed at achieving low tracking errors. In other words, since the considered scenario is static, we focus the DLL design on the use of a solution oriented to the noise reduction in order to minimize tracking errors as much as possible. Concerning the PLL, we use the optimal arctangent solution because the reference stations are not complexity limited. Concerning the PLL bandwidth selection, the choice is aimed at alleviating scintillation effects. As reflected in some papers addressing ionosphere scintillation effects [8] (and references therein), the considered PLL bandwidth usually takes values between 1 and 10 Hz. In this work, we consider a value of 3 Hz in order to attain a good trade-off in terms of noise reduction vs. tracking of the carrier phase scintillation.

ON-LINE CALIBRATION

The performance of a DBF system can be degraded by the unequal gain/phase characteristics of the RF transceiver and antenna array errors. The sources of antenna errors are the mutual coupling between radiating elements, unequal feeder gain/phase characteristics and location error. The location error can be neglected when radiating elements are mounted on a solid substrate. Those errors will result in an increased side lobe level and distorted beam shape. Therefore, the estimation and calibration of such errors is essential for the good antenna performance.

In a practical system, one of the main difficult points in a smart antenna is to calibrate the amplitude and phase of every channel over temperature and frequency. Accurate alignment of channels would require high precision hardware components and consequently a high economic cost. Thus, there is a need of a calibration system.

In order to allow performing calibration without the need of removing the antenna array to an anechoic chamber, it is intended to integrate a calibration network in the antenna structure. This network should distribute the calibration signal to each individual array element to allow the calibration of each channel stating from the output of the stacked patches up to the output of the front-end. The reference calibration signal should be injected into the main signal.

Between the antenna and the analogue-to-digital converter, the signals are amplified, mixed and filtered using analogue devices. Since the front-ends do not present exactly the same characteristics in terms of total gain and phase, it is necessary to compensate for these unbalances [9]. For this purpose, a directional coupler has been placed at the outputs of each single element and a power divider to distribute the calibration signal for the antenna has been developed.

Figure 7 shows a block diagram of the antenna system and the calibration network. The calibration network has been integrated in the same level where the directional couplers and the 180° hybrids which are necessary for producing the circular polarization of each individual element.

By using this calibration method it is possible to calculate the transfer function of each path employing correlation vectors with the reference calibration signal. The inverse of these transfer function will be the error correction coefficients. This method which injects the pilot signal in the main signal path can also calibrate the internally generated phase or amplitude errors caused by the effect of nonlinear characteristics of the RF chain [10].

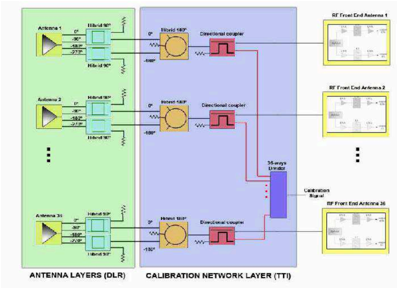

Fig. 7 Block diagram of the antenna system and the calibration network.

DIGITAL BEAMFORMING ALGORITHMS

In this section, we present the proposed digital beamforming solutions. Before doing so, however, we present the signal model considered in this paper for a better understanding of the presented algorithms.

Signal Model

The pre-correlation digital samples of the received signal at the input of the bank of correlators (see Figure 1) can be characterized with the following $Mx1$ vector:

$$\begin{aligned}\mathbf{x}_{pre}(n) &= s_{pre}(n)\mathbf{v}_{LOSS} \\ &+ \sum_{k=1}^{N_{MP}} s_{pre}\left(n - \lfloor T_{MP_k} F_{s,pre} \rfloor\right) \mathbf{v}_{MP_k} \\ &+ \sum_{k=1}^{N_I} i_k(n)\mathbf{v}_{I_k} + \mathbf{w}(n) \qquad (1)\end{aligned}$$

where $s_{pre}(n)$ stands for the Galileo signal, T_{MP_k} is the time delay of the k-th multipath component, $F_{s,pre}$ is the pre-correlation sampling frequency, i_k is the k-th interference component and $\mathbf{w}(n)$ is additive white Gaussian noise. Concerning $\mathbf{v}_{LOSS}$, $\mathbf{v}_{MP_k}$ and $\mathbf{v}_{I_k}$, these are the steering vectors corresponding to the LOSS signal, the k-th multipath component and the k-th interference component, respectively.

In the case of the signal at the output of the bank of correlators, the following expression can be adopted:

$$\begin{aligned}\mathbf{x}_{post}(n) &= s_{post}(n)\mathbf{v}_{LOSS} \\ &+ \sum_{k=1}^{N_{MP}} s_{post}\left(n - \lfloor T_{MP_k} F_{s,post} \rfloor\right) \mathbf{v}_{MP_k} \\ &+ \sum_{k=1}^{N_I} i_k(n)\mathbf{v}_{I_k} + \mathbf{w}_{post}(n) \qquad (2)\end{aligned}$$

where $F_{s,post}$ is the post-correlation sampling frequency whereas $s_{post}(n)$, $i_{post,k}(n)$ and $\mathbf{w}_{post}(n)$ stand for the Galileo signal, the k-th interference component and the noise contribution at the output of the correlators, respectively.

As observed in Figure 1, the beamformer is applied at the output of the correlators as we adopt a post-correlation beamformer. In particular, the beamforming vector is denoted by the $Mx1$ vector $\mathbf{w}(n)$ and the beamforming operation is given by the following expression:

$$y(n) = \mathbf{w}^H(n)\mathbf{x}_{post}(n)$$

Once the beamforming output is calculated, this is fed to the tracking loops of the GNSS receiver.

As previously commented, pre-correlation and post-correlation covariance estimates have to be provided to the weight control unit in accordance with the proposed beamforming solution. The pre-correlation covariance estimate can be considered as an estimate of the spatial noise-plus-interference covariance matrix because the satellite signals and the multipath signals are of very low power and are deeply buried under the noise floor. In this work, we consider the maximum likelihood estimate of the covariance matrix, which is given in case of pre-correlation covariance by [11]:

$$\hat{\mathbf{R}}_{x,pre} = \frac{1}{K}\sum_{k=0}^{K-1} \mathbf{x}_{pre}(n-k)\mathbf{x}_{pre}^H(n-k)$$

or in case of the post-correlation covariance:

$$\hat{\mathbf{R}}_{x,post} = \frac{1}{K}\sum_{k=0}^{K-1} \mathbf{x}_{post}(n-k)\mathbf{x}_{post}^H(n-k)$$

Concerning K, this is the number of snapshots considered for estimation of the pre- and post-correlation covariance matrices. In both cases, we have considered a total number of 1000 snapshots.

Finally, we conclude this subsection by describing the steering vector modelling considered in this work. Here, it is assumed that the transmission medium between the transmitter, receiver and possible scatterers is linear, non-dispersive, and isotropic such that the radiation impinging on an array of passive sensor elements can be modeled as a superposition of wavefronts generated by point sources. The point sources are located far from the array such that the direction of propagation is nearly equal at each sensor and the wavefronts are approximately planar (far-field approximation). Thus, the propagation field within the array aperture consists of plane waves. On the other hand, we also assume that the received signals are so called narrowband (array narrowband assumption, i.e., the bandwidth of the signal is much lower than the carrier frequency). With these assumptions in mind, the $Mx1$ steering vector for the

LOSS signal can be modelled as follows [11]:

$$\mathbf{v}_{LOSS} = \begin{bmatrix} 1 \\ e^{-\mathrm{j}\frac{2\pi d}{\lambda}\cos\theta\cos\phi} \\ \ldots \\ \mathrm{e}^{-\mathrm{j}\frac{2\pi d}{\lambda}(\cos\theta\cos\phi+\cos\theta\sin\phi)} \\ \ldots \\ \mathrm{e}^{-\mathrm{j}\frac{2\pi d}{\lambda}(\sqrt{M}-1)(\cos\theta\cos\phi+\cos\theta\sin\phi)} \end{bmatrix} \quad (3)$$

where λ is the carrier wavelength and θ and ϕ are the elevation and azimuth (expressed in radians) of the LOSS signal, respectively. In the case of the interference and multipath components, the steering vectors are identically computed by taking into account their associated elevation and azimuth angles. This expression takes into account the theoretical modeling of steering vectors. Real steering vectors, however, usually differ from the theoretical ones due to some perturbations found in practice. For that reason, the theoretical analysis of the proposed beamformers carried out at the first phase of ADIBEAM project (further details can be found in the Results Section) deals with the modeling of real steering vectors. To do so, the perturbation modelling described in the following subsection was adopted.

Perturbation Modelling for Theoretical Validation

The main problem arising when an antenna array is implemented in practice is the extreme difficulty to perfectly control and calibrate all the components of the system. Typical array perturbations are the non-ideal response of the hardware elements (antenna and RF chains) and mutual coupling effects. For that reason, in this work we evaluate the different beamformers at the design phase by modelling the steering vector in a way such that these phenomena are considered.

By departing from the steering vector expression presented in the previous subsection, we define a nominal steering vector $\mathbf{v}^n$, for which the m-th element can be written as follows:

$$v^n_m = g^n_m \exp\left[j\phi^n_m\right]$$

where g^n_m is the nominal gain introduced by the m-th antenna (depending on the DOA of the impinging signal) and its associated RF chain. The term ϕ^n_m is the combination of the phase delay of the impinging signal (as described in (3)) and the phase delay introduced by the hardware associated to the m-th antenna. Due to the non-idealities of the real system, the actual steering vector differs from the nominal one as follows:

$$\begin{aligned} v_m^{pert} &= \left(g^n_m + \Delta g_m\right)\exp\left[j(\phi^n_m + \Delta\phi_m)\right] \\ &= g^n_m \exp\left[j\phi^n_m\right]\left(1 + \frac{\Delta g_m}{g^n_m}\right)\exp\left[j\Delta\phi_m\right] \\ &= v^n_m \beta_m \end{aligned}$$

As observed in the previous expression, each element of the steering vector is multiplied by a perturbation factor $\beta_m = \left(1 + \frac{\Delta g_m}{g^n_m}\right)\exp\left[j\Delta\phi_m\right]$. In this work, we model the perturbation at each element as an i.i.d random variable with uniform distribution. More specifically, the gain and the phase of β_m are independently generated at each element as:

$$\left(1 + \frac{\Delta g_m}{g^n_m}\right) \sim U\ \left(10^{(-P_{gain}/10)} - 1, 10^{(P_{gain}/10)} - 1\right)$$
$$\Delta\varphi_m \sim U\ \left(-P_{phase}\pi/180, P_{phase}\pi/180\right)$$

where different values have been considered for P_{gain} and P_{phase}.

Once the perturbation errors are modelled, the coupling effect is included as well. To do so, we introduce a matrix characterizing the coupling effects, $\mathbf{C}_{coup}$, as follows:

$$\mathbf{v}^{real} = \mathbf{C}_{coup}\mathbf{v}^{pert}$$

Expressions derived above are introduced in (1) and (2) to properly characterize the received signal. By considering the DOAs of the different components of the received signal, one can easily introduce the different steering vectors.

Concerning the beamforming design, we also include some information of the hardware components (such as the measured gains, phase responses and coupling effects) to model the steering vectors. More specifically, the steering vector considered in the beamformer design is given by the following expression:

$$\mathbf{v}^{design} = \mathbf{C}_{coup}\mathbf{v}^n$$

Notice that we avoid the inclusion of perturbations in this case as these are unpredictable.

Algorithms Description

One of the main problems of the proposed scenario is the presence of multipath signals. Most of adaptive beamforming techniques fail when incoming signals are coherent or correlated. For that reason, we first propose a deterministic beamfomer aimed at cancelling the entire interference and multipath region. Furthermore, we also propose one adaptive beamformers showing a robust behaviour against coherent signals.

- DET: Deterministic Beamformer

Among the set of deterministic approaches, the most popular designs are based on conventional beamformers pointing to the direction the interest and the application of spectral weighting in order to reduce the sidelobe level response (see [11] for further details). After comparing different weighting schemes (uniform, discrete prolate spheroidal sequences, raised cosine, Kaiser, cosine weighting, Blackman-Harris and Dolph-Chebychev), one can clearly conclude that the best performance is obtained with Dolph-Chebychev weighting. However, due to the particularities of the considered scenario (attenuation of the pattern should be assured in a specific region, i.e., elevations lower than 7.5°), we have considered a deterministic approach that allows the design of desired pattern responses [12]. This scheme is based on an iterative approach and, as we will show later, better results than that obtained with Dolph-Chebychev can be achieved.

The design procedure of DET beamformer starts by defining the specification of the desired pattern. To do so, we define three parameters: the DOA of the LOSS signal (θ_d and ϕ_d), the sidelobe region of interest (Ω) and the desired response level at this region (ε). With this information in mind the algorithm is initialized as follows:

$$\begin{aligned} &\min_{\mathbf{w}} \mathbf{w}^H \mathbf{A} \mathbf{w} \\ &s.t.\;\; \mathbf{w}^H \mathbf{v}(\theta_d, \phi_d) = 1 \end{aligned}$$

where matrix $\mathbf{A} = \sum_{(\theta_i,\phi_i)\in\Omega} \mathbf{v}(\theta_i, \phi_i)\mathbf{v}^H(\theta_i, \phi_i)$ emulates the covariance matrix of a scenario with a dense set of interference signals uniformly distributed in the sidelobe region (being in our case the region covered by $0 \leq \theta \leq 7.5°$ and $0 \leq \phi \leq 360°$). In practice, this matrix is constructed by uniformly dividing the region of interest in T points. Nonetheless, we have observed in our experiments that good performance results can be obtained by selecting the identity matrix instead of matrix $\mathbf{A}$ and, by doing so, the complexity of the method is considerably reduced. It is worth noting that an additional constraint was included in the original algorithm [12] in order to assure that the maximum gain is obtained in the desired direction. However, our experiments revealed that this constraint is not needed in the considered planar array. Besides, performance is improved as two degrees of freedom are saved.

The initialization step is a constrained optimization problem with the objective of assuring a distortionless response for the desired signal and the minimization of all the directions coming from the sidelobe region Ω. Therefore, the solution can be easily obtained by means of the Lagrangian method as follows:

$$\mathbf{w}^H = \frac{\mathbf{v}^H(\theta_d, \phi_d)\mathbf{A}^{-1}}{\mathbf{v}^H(\theta_d, \phi_d)\mathbf{A}^{-1}\mathbf{v}(\theta_d, \phi_d)}$$

However, this solution does not necessarily imply a response level equal to ε in the sidelobe region. For that reason, additional iterations are included in the algorithm in order to attain the desired response. More specifically, the beamformer is updated at each iteration as follows:

$$\mathbf{w} = \mathbf{w} + \Delta\mathbf{w}$$

where $\Delta\mathbf{w}$ is the solution to the following problem:

$$\begin{aligned} &\min_{\mathbf{w}} \Delta\mathbf{w}^H \mathbf{A} \Delta\mathbf{w} \\ &s.t.\;\; \Delta\mathbf{w}^H \mathbf{v}(\theta_d, \phi_d) = 0 \\ &\qquad \Delta\mathbf{w}^H \mathbf{v}(\theta_j, \phi_j) = f_j \qquad \text{for } j = 1..M-1 \end{aligned}$$

The above constraints are imposed to assure that the distortionless property is maintained ($(\mathbf{w}+\Delta\mathbf{w})^H\mathbf{v}(\theta_d, \phi_d) = 1$ if $\Delta\mathbf{w}^H\mathbf{v}(\theta_d, \phi_d) = 0$) and that the directions in the region Ω with the highest response (denoted as $\mathbf{v}(\theta_j, \phi_j) = f_j,\; j = 1..M-1$) attain the desired response. To do so, f_j is computed as $f_j = (\varepsilon - |c_j|)c_j / |c_j|$, being c_j the response to the previous beamformer $\mathbf{w}^H\mathbf{v}(\theta_j, \phi_j) = c_j$. Then, by defining matrix

$$\mathbf{C} = [\mathbf{v}(\theta_d, \phi_d), \mathbf{v}(\theta_1, \phi_1), ..., \mathbf{v}(\theta_{M-1}, \phi_{M-1})]$$

and vector $\mathbf{g} = [0, f_1, ..., f_{M-1}]^T$, the following solution is obtained for $\Delta\mathbf{w}$:

$$\Delta\mathbf{w}^H = \mathbf{g}^H \left(\mathbf{C}^H\mathbf{A}^{-1}\mathbf{C}\right)^{-1} \mathbf{C}^H\mathbf{A}^{-1}$$

With the obtained result, the beamforming vector is updated and the algorithm is iterated until convergence. In situations where convergence is attained, the number of required iterations depends on the target pattern response but it is usually of the order of the number of antennas.

It is worth recalling that this is a deterministic beamformer. Then, the beamforming solution for the different LOSS DOAs can be computed off-line and saved.

- IAA: Iterative Adaptive Algorithm

The Iterative Adaptive Approach (IAA) method is an adaptive beamformer based on a robust design criterion. This algorithm was selected due to its good behavior in terms of robustness as reported in [6]. More specifically, the authors in [6] compared the IAA beamformer with other robust approaches and showed that this option is the most equilibrated strategy in terms of SINR, estimation accuracy of DOA and power of the desired signal.

Further details of the algorithm can be found in [6] but basically the idea consists in defining a scanning grid of L directions by constructing a set of L steering vectors $\mathbf{V} = [\mathbf{v}(\theta_1, \phi_1), ..., \mathbf{v}(\theta_L, \phi_L)]$. Once this scanning grid is defined, the algorithm estimates the powers at each direction and gathers them in matrix $\hat{\mathbf{P}} = diag\{\hat{P}_1, ..., \hat{P}_L\}$. After that, the beamformer for each direction (θ_l, ϕ_l) (with a potential source) is computed as:

$$\mathbf{w}_l^H = \frac{\mathbf{v}^H(\theta_l, \phi_l)\bar{\mathbf{R}}^{-1}}{\mathbf{v}^H(\theta_l, \phi_l)\bar{\mathbf{R}}^{-1}\mathbf{v}(\theta_l, \phi_l)}$$

where $\bar{\mathbf{R}}$ is a estimate of the covariance matrix iteratively computed by considering the received signal $\mathbf{x}(n)$ for N snapshots as follows:

$$\hat{s}_l(n) = \mathbf{v}^H(\theta_l, \phi_l)\mathbf{x}(n)/M \qquad n = 1..N; l = 1..L$$

$$\hat{P}_l = \frac{1}{N}\sum_{n=1}^{N} |\hat{s}_l(n)|^2 \qquad l = 1..L$$

repeat

$$\bar{\mathbf{R}} = \mathbf{V}\hat{\mathbf{P}}\mathbf{V}^H$$

for $l = 1..L$

$$\mathbf{w}_l^H = \frac{\mathbf{v}^H(\theta_l, \phi_l)\bar{\mathbf{R}}^{-1}}{\mathbf{v}^H(\theta_l, \phi_l)\bar{\mathbf{R}}^{-1}\mathbf{v}(\theta_l, \phi_l)}$$

$$\hat{P}_l = \mathbf{w}_l^H \hat{\mathbf{R}}_x \mathbf{w}_l$$

end

until convergence

Notice that the beamforming solution is similar to the MPDR approach and the robustness against array perturbations and coherent signals comes from two facts: 1) matrix $\hat{\mathbf{P}}$ is defined by considering that the sources are uncorrelated, and 2) the covariance matrix is estimated by taking into account the power arriving from the directions where the different beamformers are pointing at, being this power estimate obtained by taking into account the sample covariance matrix $\hat{\mathbf{R}}_x$. It is worth noting that we analyzed IAA by considering both the pre- and post-correlation covariance matrices and the best results were obtained with the former case. For that reason, we consider the pre-correlation version of IAA in the sequel (i.e., IAA working with the pre-correlation covariance matrix).

EXPERIMENTATION PLATFORM

In Fig. 8, we present the block diagram of the Experimentation Platform developed in ADIBEAM project. As observed, this software platform is divided into two blocks: the signal generator and the GNSS software receiver. Next, we describe these blocks with more detail.

Signal Generator

The Signal Generator emulates GNSS signals as they would appear in a real receiver after the receiver antenna and front-end (see Fig. 8). The simulated GNSS signals are the L1 and E5b signals related to the SoL (Safety of Life) services. The signals are generated in a complex baseband representation. The simulator implements different propagation channel effects affecting the GNSS signal like scintillation, Doppler variation and multipath. Furthermore the generator takes in account several aspects pertaining to the antenna and receiver chain like the single antenna radiation pattern, antenna and array imperfections, antenna array mutual coupling, front-end filtering, ADC quantization, reference clock instability and AWGN. Radio frequency interferers are also simulated and fed in the receiver chain without being affected by the propagation channel.

The software allows selecting different directions of arrival for the LOSS signal and for each of the multipaths and interferers. The interferers are supposed to be ground-based and therefore an elevation lower than 7.5° has been considered. Multipath amplitudes and phases are random values following a gamma and a uniform distribution, respectively.

The scintillation simulation implements amplitude fading and phase variations based on a Nakagami-m and zero-mean Gaussian distribution respectively. Nakagami-m distribution is generated based on a trivariate gamma distribution. Scintillation parameter S4 and phase standard deviation $\sigma_{\delta\phi}$ are extrapolated using the Wideband Ionospheric Scintillation model (WBMOD) considering a sunspot number equal to 140, a receiver position close to the equatorial region, a Kp value of 4 and a receiver time starting from sunset to midnight.

GNSS signals are formed by a repetition of a reference band-limited pulse, whose form depends on the channel modulation. The output of the signal generator are binary files, one for each of the radiating element composing the antenna array.

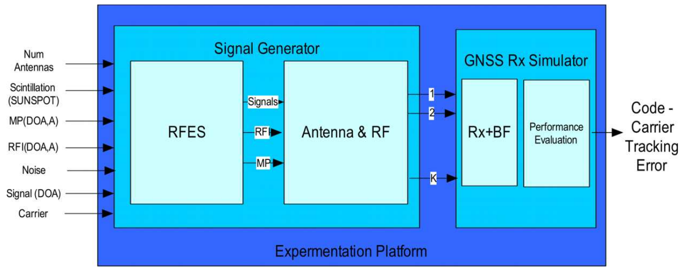

Fig. 8 Block diagram of the Experimentation Platform.

GNSS Software Receiver

In Fig. 9 the architecture of the GNSS Receiver Subsystem simulator is presented. This subsystem receives the K signals processed by the Antenna and RF Subsystem (as would be received by K real receive elements) and applies the digital beamforming and GNSS reception algorithms described in the previous sections. As a final step, a performance evaluation block is also included in the GNSS Receiver Subsystem. In this block, statistics regarding code and carrier tracking error (bias and standard deviation) are obtained.

Like the signal generator, this part of the simulator has been implemented in MATLAB. Even though the simulator is not operating in real time, the implementation has been carefully designed so that the resulting tool is suitable and flexible enough for the experimentation. Further details of the general architecture of the GNSS receiver and the implementation of the digital beamforming are depicted

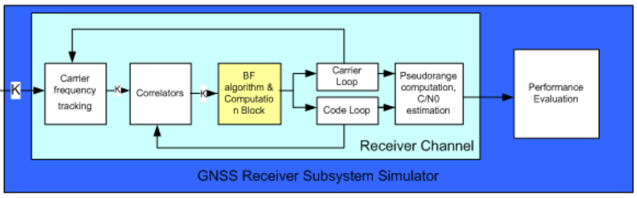

Fig. 9 GNSS Receiver Subsystem simulator.

in Fig. 10. Since this project considers deterministic and adaptive beamforming algorithms, the receiver has been designed to be flexible enough to process both algorithms and receive different inputs.

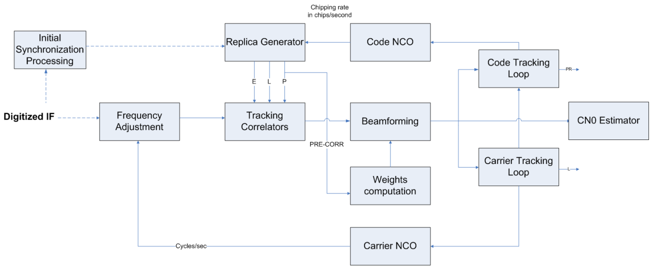

Fig. 10 GNSS Receiver Architecture.

In the calibration procedures at the antenna and front-end levels, phase and gain responses are estimated and this information is passed to the GNSS receiver and the beamforming algorithm in order to be compensated in the signal processing part.

As a conclusion, the receiver block has been designed by taking into account the following:

- Beamforming integration in order to take advantage of the advantages of a multi-antenna receiver.
- Conventional tracking blocks in order to make easier their implementation and optimization.
- Optimization of the code related to the beamforming algorithms in order to minimize computational complexity.
- Flexibility from algorithm and configuration point of view.

ADIBEAM RESULTS

In this section, we present the main results obtained in the ADIBEAM project. It is worth noting that the project was divided in two phases: design phase and experimentation phase. In the first phase, the beamformers were analyzed from a theoretical point of view in order to pre-evaluate them and adapt the algorithms design. After that, the algorithms were implemented in the Experimentation Platform for a more realistic validation. Next, we provide results corresponding to the two phases.

Table 1 Tracking Errors for DET beamformer (36 antennas, L1).

	DLL errors (cm)	PLL errors (mm)
S1 (10°)	5.5	3.4
S2 (10°)	6.0	3.5
S1 (30°)	2.2	1.2
S2 (30°)	2.7	1.2

Theoretical Results

In the design phase, we tested the algorithms by adopting theoretical expressions for the DLL and PLL tracking errors in accordance with the array gain and attenuation provided by the different solutions. However, all the components of the receiver system were considered in order to provide more realistic results (as described in the Perturbation Modelling subsection). In particular, we considered most of the parameters adopted in the experimentation platform (antenna patterns, RF chains, coupling matrix, GNSS receiver parameters) and the main difference here is that the signals are not processed. Instead, the statistical values for DLL and PLL errors are obtained.

In order to analyze the behavior of the algorithm, several scenarios were considered. In this paper, however, results are presented for two possible LOSS elevations ($\theta = 10°$ and $\theta = 30°$) and only one LOSS azimuth equal to $\phi = 90°$. Besides, we focus on two scenarios:

- Scenario 1 (S1): only multipath signals.
- Scenario 2 (S2): multipath signals and two interference signals (weak signal at $\theta = 7.5°$ and $\phi = 180°$, strong signal at $\theta = 3°$ and $\phi = 135°$).

where we consider the following:

- Presented results consider the averaging of simulations results with different multipath realizations. In particular, each realization considers random multipath elevations (between 0 and $7.5°$) and azimuths (between $-40°$ and $40°$ with respect to the LOSS azimuth).
- As commented above, some experiments revealed that the IAA beamformer based on pre-correlation covariance matrix works better than its post-correlation counterpart. For that reason, we focus on the pre-correlation IAA beamformer.

We start by presenting in Table 1 results corresponding to DET beamformer for L1 band. As observed results in the order of cm and mm are attained for DLL and PLL errors, respectively. Therefore, beamforming is a very useful

Table 2 Tracking Errors for DET beamformer (36 antennas, E5b).

	DLL errors (cm)	PLL errors (mm)
S1 (10°)	2.3	5.8
S2 (10°)	2.5	5.8
S1 (30°)	2.0	0.4
S2 (30°)	2.0	0.4

Table 3 Tracking Errors for IAA beamformer (36 antennas, L1).

	DLL errors (cm)	PLL errors (mm)
S1 (10°)	6.2	2.9
S2 (10°)	6.7	2.9
S1 (30°)	2.4	0.8
S2 (30°)	2.8	0.8

strategy to satisfy the high accuracy demands of Galileo ground stations. One can also observe that better results are obtained when the LOSS elevation is higher. This is because there exists a higher separation between the LOSS signal and the region where the attenuation is introduced. Then, the beamresponse is not so deteriorated and the array gain is not penalized. In Table 2, we present results corresponding to the E5b band. When compared to the L1 case, it is observed that results are better in terms of DLL errors. This is because E5b spreading gain is higher as so is the chip rate. Concerning PLL errors, better results are obtained with L1 because of its lower wavelength.

In Tables 3 and 4, we present results for the IAA beamformer corresponding to the L1 and E5b bands, respectively. As observed, satisfactory results are also obtained but DET performance is generally better. Nevertheless, the performance gap between both solution is small, so any of the two methods (IAA or DET) is a valid and powerful solution for the proposed scenario. Besides, we should point out that IAA is an adaptive solution able to properly work in the case that scenario characteristics are modified.

Experimentation Platform Preliminary Results

First of all, it is worth noting that the experimentation phase is still under development. For that reason, this subsection focuses on providing preliminary results obtained with the experimental tool described in the previous sections. In particular, we present results for the following scenario:

- L1 band.
- LOSS DOA equal to $\theta = 30°$ and $\phi = 90°$.
- Uniform rectangular array with 4 antennas.
- Four multipath signals with constant DOAs ($\theta_1 = 5°$, $\phi_1 = 140°$, $\theta_2 = 3°$, $\phi_2 = 130°$, $\theta_3 = 7°$, $\phi_3 = 120°$, $\theta_4 = 4°$, $\phi_4 = 110°$) and two interference signals (weak signal at $\theta = 5°$ and $\phi = 125°$, strong signal at $\theta = 2°$ and $\phi = 135°$).

Table 4 Tracking Errors for IAA beamformer (36 antennas, E5b).

	DLL errors (cm)	PLL errors (mm)
S1 (10°)	3.5	4.5
S2 (10°)	3.8	4.6
S1 (30°)	3.0	2.7
S2 (30°)	3.6	2.8

Table 5 Tracking Errors obtained with the Experimental Platform (4 antennas, L1).

	DLL errors (cm)	PLL errors (mm)
Single Antenna	196	0.8
DET	36	0.95
IAA	45	0.75

In Table 5, we compare results obtained with DET and IAA with those obtained with a single antenna receiver. Before discussing these results, it is worth noting that it has been observed in the project that DLL errors strongly depends on the array gain, whereas PLL results are driven by the level of attenuation provided by the beamformer. For that reason, errors in terms of DLL are significantly reduced when adopting digital beamforming solution due to the gain provided by the multiple antenna receiver. Concerning PLL errors, however, similar results are obtained with and without an array of antennas. This is because a planar array with only four antennas is considered here and the receiver is not very efficient to provide a good level of attenuation in a scenario with a low LOSS elevation.

Finally, it is worth recalling that results provided here are preliminary results in order to verify the well behavior of the implemented Experimental Platform. Consequently, several tests must be performed in order to consolidate the final results of the project.

CONCLUSIONS

In this paper, we have presented the receiver design proposed in the ESA-funded project ADIBEAM aimed at providing Galileo with high accuracy ground stations. This design is based on the use of an array of antennas and digital beamforming. In order to address the problems found in practice and efficiently combating array perturbations, robust beamforming solutions have been proposed. The proposed solutions have been validated in different scenarios, showing that cm and mm level accuracy can be obtained for code and carrier phase tracking, respectively. Besides, an Experimental Platform emulating all the elements of a real receiver has been implemented. For this case, preliminary results have been presented proving the validity of the proposed multi-antenna receiver.

REFERENCES

[1] F. Amarillo, A. Ballereau, M. Crisci, B. Lobert, and S. Lannelongue, "Galileo IOV ground mission segment performances," *in Proc. GNSS ENC*, 2008.

[2] G. Seco-Granados, J. A. Fernandez-Rubio, and C. Fernandez-Prades, "Ml estimator and hybrid beamformer for multipath and interference mitigation in gnss receivers," *IEEE Trans. on Signal Processing*, vol. 53, pp. 1194–1208, March 2005.

[3] S. Backen, D. Akos, and M.L. Nordenvaad, "Post-processing dynamic GNSS antenna array calibration and deterministic beamforming," *in Proc. of the 21st International Technical Meeting of the Satellite Division of the ION (ION GNSS 2008), Savannah*, 2008.

[4] K.A. Griffith and I.J. Gupta, "Effect of mutual coupling on the performance of gps aj antennas," *Navigation*, vol. 56, pp. 161–173, 2009.

[5] C.-L. Chang and J.-C. Juang, "A new pre-processing approach against array uncertainty for gnss," *Proc. of IEEE/ION PLANS*, 2008.

[6] L. Du, T. Yardibi, J. Li, and P. Stoica, "Review of user parameter-free robust adaptive beamforming algorithms," *Digital Signal Processing*, vol. 19, pp. 567–582, 2009.

[7] E. N. Lavado, M. V.T. Heckler, W. Elmarissi, and A. Dreher, "Dual-band microstrip antenna for a robust navigation receiver," *Proc. of ENC-GNSS*, 2009.

[8] T. N. Morrissey, K. W. Shallberg, A. J. Van Dierendonck, and M. J. Nicholson, "GPS receiver performance characterization under realistic ionospheric phase scintillation environments," *Radio Science*, vol. 39, 2004.

[9] M. V. T. Heckler, W. Elmarissi, L. A. Greda, M. Cuntz, and A. Dreher, "Narrowband microstip antenna array for a robust receiver for navigation applications," *3rd European Conference of Antennas and Propagation*, 2009.

[10] D. H. Lee and C. S. Pyo, "Performance and effect of calibration in smart antenna system," *Radio Technology Research Group, ETRI (Electronics and Telecommunication Research Institute)*, 2004.

[11] H.L. Van Trees, *Optimum Array Processing (Detection, Estimation and Modulation Theory, Part IV)*, John Wiley, 2002.

[12] C-Y. Tseng and L. J. Griffiths, "A simple algorithm to achieve desired patterns for arbitrary arrays," *IEEE Trans. on Signal Processing*, vol. 40, pp. 2737–2746, Nov. 1992.